

Phase diagram of QCD with four quark flavors at finite temperature and baryon density

Vicente Azcoiti^{a*}, Giuseppe Di Carlo^{b†}, Angelo Galante^{b,c‡}, Victor Laliena^{a§}

^a *Departamento de Física Teórica, Universidad de Zaragoza,
Pedro Cerbuna 12, E-50009 Zaragoza (Spain)*

^b *INFN, Laboratori Nazionali del Gran Sasso, 67010 Assergi (L'Aquila) (Italy)*

^c *Dipartimento di Fisica dell'Università di L'Aquila 67100 L'Aquila (Italy)*

April 27, 2005

Abstract

We analyze the phase diagram of QCD with four staggered flavors in the (μ, T) plane using a method recently proposed by us. We explore the region $T \gtrsim 0.7 T_C$ and $\mu \lesssim 1.4 T_C$, where T_C is the transition temperature at zero baryon density, and find a first order transition line. Our results are quantitatively compatible with those obtained with the imaginary chemical potential approach and the double reweighting method, in the region where these approaches are reliable, $T \gtrsim 0.9 T_C$ and $\mu \lesssim T_C$. But, in addition, our method allows us to extend the transition line to lower temperatures and higher chemical potentials.

*E-mail: azcoiti@azcoiti.unizar.es

†E-mail: dicarlo@lngs.infn.it

‡E-mail: galante@lngs.infn.it

§E-mail: laliena@unizar.es

1 Introduction

The study of QCD at finite baryon density is one elusive problem of utmost importance for the understanding of strong interactions. Many features of the behavior of hadronic and quark matter at high baryon density have been suggested mainly from the analysis of effective theories. On this basis, a rich structure of phases and phase transitions is expected, and the dependence of the phase structure on the quark masses has been conjectured [1]. Unfortunately, the sign problem prevents the direct use of Monte Carlo simulations at finite baryon density. However, in the last years methods to get the transition line at high temperature and low baryon density, overcoming the sign problem, have been proposed. One method uses double reweighting (in the two parameters, β and μa) of the configurations generated at the transition temperature at zero chemical potential, following the transition line in the $(\mu a, \beta)$ plane [2]. The rationale of this method is that it is expected that the overlap between the reweighted ensemble and the ensemble at a given point of the transition line will be improved respect to the Glasgow method [3], since the original ensemble is itself a mixture of configurations corresponding to the confined and deconfined phase. This approach has been used in a first attempt to locate the expected critical endpoint of QCD with 2+1 flavors by using only first principles [4]. Another method exploits the well known fact that there is no sign problem if the chemical potential is purely imaginary [5]. Then, it was realized in [6] that it is possible to determine, by means of numerical simulations, a pseudo-transition line at imaginary chemical potential and extend it analytically to real chemical potential. This method has been used to study the phase diagram at small chemical potential around the zero density transition point in QCD with two and three degenerate quark flavors in [6] and with four flavors in [7]. Another proposal that is being employed to extract information about the phase transition in the region of small chemical potential is to compute the expectation values of the derivatives respect to μa at $\mu a = 0$, in order to reconstruct several terms of the Taylor series [8, 9].

Recently we devised another method which can be regarded as a generalization of the imaginary chemical potential approach. The former has several advantages over the later, for it seems that it can be used to determine the transition line at lower temperatures and higher densities [10]. Especially interesting is the fact that it may be used to locate the critical endpoint expected in two flavor QCD [11].

In this paper we report the results of the phase transition line of lattice QCD with four degenerate flavors of staggered quarks obtained with this new method. At zero density a very clear first order transition separates the low and high temperature phases, at a transition temperature, T_C , that, for small quark masses, ranges from 100 MeV to 170 MeV [12]. It is expected that the transition continues along a line in the (μ, T) plane, with the transition temperature lowering as μ increases. This is what has been obtained using the double reweighting [2] and the imaginary chemical potential [7] approaches. We also find a first order transition line starting at $\mu = 0$ and $T = T_C$ and continuing at lower temperatures as μ increases. Our results are quantitatively compatible with those obtained in [7] with the imaginary chemical potential approach and with the results of the double reweighting method [2], in the region where these approaches are reliable (see sections three and four for a discussion on this point). But, in addition, our method allows us to extend the transition line to lower temperatures and higher chemical potentials.

The remaining of the paper is organized as follows: in next section we explain our approach. In section three we describe the numerical results and in section four we present our conclusions.

2 Review of the method

The numerical method used in this work is based on the definition of a generalized QCD action which depends on two free parameters (x, y) . This generalized action suffers also from the sign problem for real values of y but not for imaginary values of it. Simulations will be then performed at imaginary values of y and at the end analytical extensions will be needed. The main advantage of this approach when compared with the imaginary chemical potential method is that we can explore the phase transition line at imaginary values of y at any given physical temperature i.e., we are not forced, as in the case of imaginary chemical potential, to perform simulations at so high temperatures that the system is in the quark-gluon plasma phase for any real value of μa . In this section we shall describe this method. The interested reader can find more details of it in [10].

The lattice action for QCD with staggered fermions and chemical potential μ is

$$S = S_{\text{PG}} + \frac{1}{2} \sum_n \sum_{i=1}^3 \bar{\psi}_n \eta_i(n) \left(U_{n,i} \psi_{n+i} - U_{n-i,i}^\dagger \psi_{n-i} \right) + \frac{1}{2} \sum_n \bar{\psi}_n \eta_0(n) \left(e^{\mu a} U_{n,0} \psi_{n+0} - e^{-\mu a} U_{n-0,0}^\dagger \psi_{n-0} \right) + ma \sum_n \bar{\psi}_n \psi_n, \quad (1)$$

where S_{PG} is the standard Wilson action for the gluonic fields, which contains β , the inverse gauge coupling, as a parameter, $\eta_i(n)$ and $\eta_0(n)$ are the Kogut-Susskind phases, m the fermion mass, and a the lattice spacing.

Let us now define the following generalized action

$$S = S_{\text{PG}} + ma \sum_n \bar{\psi}_n \psi_n + \frac{1}{2} \sum_n \sum_{i=1}^3 \bar{\psi}_n \eta_i(n) \left(U_{n,i} \psi_{n+i} - U_{n-i,i}^\dagger \psi_{n-i} \right) + S_\tau(x, y), \quad (2)$$

with

$$S_\tau(x, y) = x \frac{1}{2} \sum_n \bar{\psi}_n \eta_0(n) \left(U_{n,0} \psi_{n+0} - U_{n-0,0}^\dagger \psi_{n-0} \right) + y \frac{1}{2} \sum_n \bar{\psi}_n \eta_0(n) \left(U_{n,0} \psi_{n+0} + U_{n-0,0}^\dagger \psi_{n-0} \right), \quad (3)$$

where x and y are two independent parameters. The QCD action is recovered by setting $x = \cosh(\mu a)$ and $y = \sinh(\mu a)$.

Monte Carlo simulations of the model (2) for real values of x, y are not feasible since we meet the sign problem. However if y is a pure imaginary number, $y = i\bar{y}$, where \bar{y} is real, the sign problem disappears since the fermionic matrix is the sum of a constant diagonal

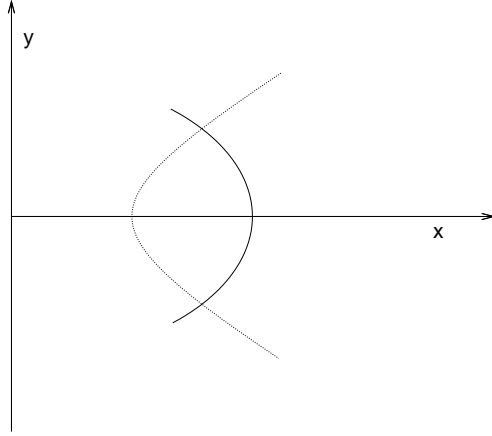


Figure 1: Minimal phase diagram conjectured for the generalized QCD. The solid line is line of phase transitions. The discontinuous line is the physical line, $x^2 - y^2 = 1$.

matrix plus an antihermitian matrix which anticommutes with the staggered version of the γ_5 Dirac matrix, and numerical simulations become feasible. Imaginary chemical potential is a particular case of this, obtained by setting $x = \cos(\mu a)$ and $\bar{y} = \sin(\mu a)$.

The expected phase diagram for this model in the (x, y) plane is shown in Fig. 1 [10]. The solid line is a presumed line of phase transitions and the discontinuous line is the physical line, $x^2 - y^2 = 1$, along which one recovers standard QCD at finite baryon density. The intersection of the solid line with the discontinuous one will therefore give us the transition chemical potential of QCD at a given temperature. A change in the physical temperature can be simulated by changing β keeping fixed L_t or vice-versa. In both cases the solid line in Fig. 1 will move and the intersection point which gives the transition chemical potential will change with the physical temperature. For small β the transition line crosses the $y = 0$ axis at $x > 1$ and, therefore, intersects the physical line also at $x > 1$, producing a physical phase transition at $\mu a > 0$. By increasing β and keeping fixed the temporal lattice extent L_t , the transition point on the $y = 0$ axis moves toward $x = 1$ and eventually crosses it. Clearly, the value of β at which the transition line intersects the physical line at $x = 1$ and $y = 0$ is the zero density transition point. For larger β the transition line and the physical line do not intersect and the system is in the deconfined phase whatever the chemical potential.

From an analysis of the symmetries of the action (2) it is not difficult to realize that the partition function depends on x and y only through the combinations

$$\begin{aligned} u &= x^2 - y^2, \\ v &= (x + y)^{3L_t} + (x - y)^{3L_t}. \end{aligned} \quad (4)$$

For imaginary values of y ($y = i\bar{y}$) we have $u = \rho^2$ and $v = 2\rho^{3L_t} \cos(3L_t\eta)$, where $\rho^2 = x^2 + \bar{y}^2$ and $\tan \eta = \bar{y}/x$, and, therefore, the free energy will be a periodic function of η with period $2\pi/3L_t$. In particular if the phase transition line of Fig. 1 continues to imaginary values of y , the expected phase diagram in the (x, \bar{y}) plane is displayed in Fig.

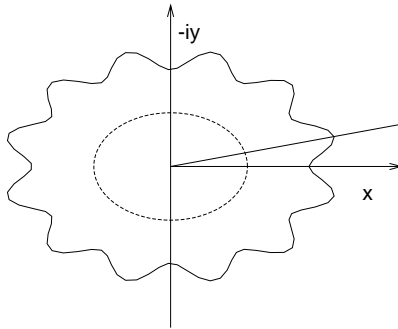


Figure 2: Conjectured phase diagram in the (x, \bar{y}) plane. We have incorporated the periodicity. The dashed line contains the points corresponding to imaginary chemical potential.

2, where we have incorporated the property of periodicity. In Fig. 2 we have also included the line $\rho = 1$ (dotted) which is the locus of the points accessible to numerical simulations of QCD at imaginary chemical potential. One can see now how this approach has more potentialities than the imaginary chemical potential approach. Indeed by increasing the inverse gauge coupling β , the phase transition line of Fig. 2 moves toward the origin of coordinates. In some interval (β_m, β_M) the transition line intersects the $\rho = 1$ line and then a phase transition will appear at imaginary chemical potential. In such a situation, the physical temperature is so high that the system is in an unconfined phase for any real value of the chemical potential. The advantage of our approach is that in our simulations ρ is not enforced to be one.

The variables u and v have the interesting property that are real for both y real and pure imaginary, so that they map the two planes (x, y) and (x, \bar{y}) onto a single plane (u, v) . The line $v = 2u^{3L_t/2}$ separates the regions corresponding to each plane: the region above it in Fig. 3 corresponds to real y and is not accessible to numerical simulations, while the region below it corresponds to imaginary y and can be explored by means of simulations. The physical line is $u = 1$ with $v \geq 2$. The imaginary chemical potential points are mapped onto the line $u = 1$, $-2 \leq v \leq 2$. The analytical extension from imaginary y to the physical real y becomes in the (u, v) plane the extrapolation from the region accessible to numerical simulations to $u = 1$, $v \geq 2$.

In order to get the transition chemical potential we must determine the coordinates of the intersection point between the solid line and the physical line in Fig. 1. From the symmetries of the partition function we know that the phase transition line is an even function of x and y . Therefore, we can write the following equation for the transition line at fixed β in the (x, y) plane¹

$$x^2 = 1 + a_0(\beta) + a_2(\beta)y^2 + a_4(\beta)y^4 + O(y^6), \quad (5)$$

By fixing the lattice temporal extent L_t and the gauge coupling β one fixes the physical

¹Here and in the following we do not write explicitly the dependence of the coefficients a_i, β_0, b_i , etc. on the temporal lattice extent, L_t , and the quark masses, ma .

temperature T . The intersection point of the transition line with the physical line

$$y_c^2 = a_0(\beta) + a_2(\beta)y_c^2 + a_4(\beta)y_c^4 + O(y_c^6), \quad (6)$$

will give us the transition chemical potential, $y_c = \sinh(\mu_c a)$, at this temperature.

The strategy for the determination of the transition chemical potential is then the following. From numerical simulations at imaginary values of y , $y = i\bar{y}$, near the phase transition point $((1 + a_0)^{1/2}, 0)$ one can locate several phase transition points in the (x, \bar{y}) plane (see Fig. 2). By fitting these points with equation (5) with the + sign of the coefficient proportional to y^2 replaced by $-$, we can numerically measure the first coefficients. Ignoring the quartic term, the transition chemical potential, $\mu_c a$, will then be given by

$$\mu_c a = \pm \sinh^{-1} \left(\frac{a_0}{1 - a_2} \right)^{1/2}. \quad (7)$$

An alternative procedure, which is indeed the one employed in this work, is to project of the phase diagram onto the (y, β) plane. In practice, we fix $x = x_0 > 1$, L_t and the lattice quark masses² and perform simulations for different values of \bar{y} and β . In this way we can easily find an accurate estimate of the transition point at a given \bar{y} by interpolation in β via reweighting. The qualitative phase diagram in the (y, β) plane is displayed in Fig. 4. The solid lines are the physical lines,

$$y = y_{\text{ph}} = \pm \sqrt{x_0^2 - 1}, \quad (8)$$

and the discontinuous line is a line of phase transitions.

Using again the symmetries of the partition function we can write for this line the following equation

$$\beta = \beta_0(x_0) + b_2(x_0)y^2 + O(y^4). \quad (9)$$

As in the case discussed previously, one can measure β_0 and b_2 from simulations at $y = 0$ and at imaginary $y = i\bar{y}$ (keeping x_0 fixed). Then, we have to find the intersection point between the physical and phase transition lines of Fig. 4.

Equivalently, one may use the plane (u, β) , where $u = x_0^2 + \bar{y}^2 > 1$. From simulations at fixed $x = x_0$ and $\bar{y} \geq 0$ we can get a phase transition line $\beta(u)$ for $u \geq x_0^2 > 1$. Then one can extrapolate this line to $u = 1$, thus obtaining the physical transition coupling at chemical potential $\mu a = \cosh^{-1}(x_0)$.

3 Numerical results

We performed simulations of QCD with four degenerate flavors of staggered quarks using the Hybrid Monte Carlo algorithm on lattices of sizes $6^3 \times 4$ and $8^3 \times 4$. Our method is computationally very expensive and it is rather difficult to go to larger lattices. The quark mass in lattice units was fixed to $ma = 0.05$. On each lattice, we repeated the simulations for several values of x , \bar{y} , and β . We measured the plaquette, the chiral condensate, and the Polyakov loop after each molecular dynamics trajectory of unit time. For each simulation we accumulate between thirty and forty thousand measurements. Most of the

²Notice that in the imaginary chemical potential approach x_0 is enforced to be less than one.

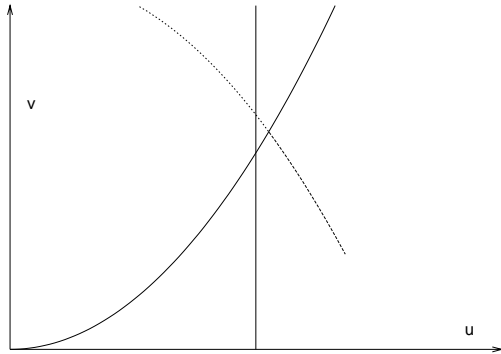


Figure 3: Phase diagram in the (u, v) plane. The solid line, $v = 2u^{3L_t/2}$ corresponds to $y = 0$, and separates the region where numerical simulations are feasible (below the line) from the region where the sign problem prevents numerical simulations (above the line). The discontinuous line is a hypothetical phase transition line. The line $u = 1$ is also displayed. For $v \geq 2$ it is the physical line while for $-2 \leq v \leq 2$ it corresponds to imaginary chemical potential.

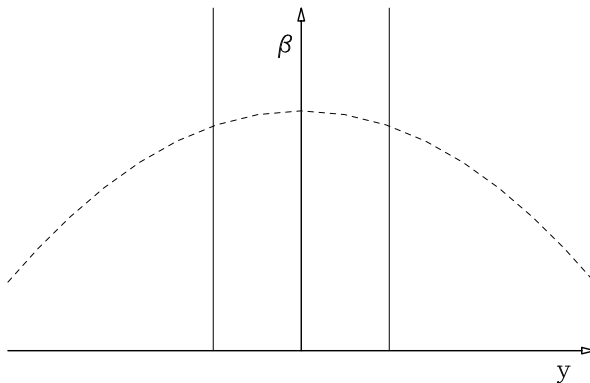


Figure 4: Conjectured phase diagram in the (y, β) plane, with $x = x_0 > 1$ fixed. The discontinuous line is a line of phase transitions, whereas the solid lines are the physical lines, $y = y_{\text{ph}} = \pm\sqrt{x_0^2 - 1}$.

simulations have been performed on the Linux clusters of LNGS-INFN, and some of them in the Linux cluster of Departamento de Física Teórica of Universidad de Zaragoza.

At zero chemical potential ($x = 1$ and $\bar{y} = 0$) there is a very clear signal of a first order phase transition controlled by β , at which the plaquette, the chiral condensate, and the Polyakov loop vary abruptly and show a clear two state structure. This first order transition persists for $x > 1$ and $\bar{y} \geq 0$, with the transition coupling depending on x and \bar{y} . To determine the transition lines numerically, we proceeded as follows. For each pair (x, \bar{y}) we estimate the transition coupling by reweighting *à la* Ferrenberg-Swendsen (in the parameter β) the configurations corresponding to the value of β at which a clear two state signal appeared. We used the maximum of the plaquette susceptibility as the criterion to define the transition coupling on the finite lattice, since it gives the best signal.

In this way, for each value of x we have a transition line in the plane (\bar{y}, β) . We fit this line with a second order polynomial:

$$\beta(\bar{y}) = \beta_0(x) + b_2(x)\bar{y}^2. \quad (10)$$

L	x	β_0	β_{ph}	b_2	χ^2/ndof	ndof
6	1.02	5.0359(2)	5.008(1)	0.68(2)	0.4	1
6	1.045	5.028(1)	4.962(3)	0.72(3)	1.63	1
8	1.0201	5.0367(5)	5.0089(10)	0.684(15)	0.82	4
8	1.0314	5.0332(3)	4.9869(12)	0.726(13)	1.11	5
8	1.0453	5.0292(5)	4.9636(21)	0.708(21)	0.97	5
8	1.0811	5.0179(4)	4.8943(20)	0.732(10)	0.36	7
8	1.1276	5.0047(4)	4.8017(28)	0.747(9)	0.97	6

Table 1: Parameters of the χ^2 fits of the transition lines in the (\bar{y}, β) [or (u, β)] plane for different values of x , extracted from simulations on the $L = 6$ and $L = 8$ lattices.

The analytic continuation of this functions to real $\bar{y} = -iy$ is trivial:

$$\beta(y) = \beta_0(x) - b_2(x)y^2. \quad (11)$$

The physical value of y is $y_{\text{ph}} = \sqrt{x^2 - 1}$. Hence, the physical transition coupling is $\beta(y_{\text{ph}}) = \beta_0(x) - b_2(x)(x^2 - 1)$.

We can also use the variable $u = x^2 + \bar{y}^2$, and then the transition line in the plane (u, β) is fit by the linear function

$$\beta(u) = \beta_{\text{ph}}(x) + b_2(x)(u - 1). \quad (12)$$

Notice that the fits in the (\bar{y}, β) and (u, β) are identical since both the data and the fit functions are related by the same transformation. In the (u, β) plane the analytic continuation to $\bar{y} = -iy_{\text{ph}}$ corresponds to the extrapolation to $u = 1$. Hence, the physical transition coupling for each value of x is directly given by the parameter β_{ph} .

Table I collects the parameters of the best χ^2 fits of the transition lines given by equations (10) or (12) extracted from simulations on the $6^3 \times 4$ and $8^3 \times 4$. The transition lines at fixed x are displayed in Figures 5 and 6. The left panels represent the (\bar{y}, β) plane, for the open symbols and the dashed line, and the (y, β) plane, for the solid and dotted lines, and the filled circle. The right panels represent the (u, β) plane. In all plots the open symbols are the numerical estimates of the phase transition points obtained from the simulations on the $8^3 \times 4$ lattice. On the left panels, the dashed line is the best χ^2 fit to a function of the form (10) and the solid line is its analytical continuation to $y = iy$. The dotted line is the physical line, given by $y = y_{\text{ph}} = \sqrt{x^2 - 1}$, and the filled circle is the physical transition point. On the right panels, the solid line is the fit of the transition points to a function of the form (12) and the dashed line is the boundary of the region where numerical simulations without sign problem can be performed (i.e., the line $u = x^2$). The filled circle is the physical transition point obtained extrapolating the transition line to the physical region, $u = 1$.

In the transition lines displayed in Fig. 6 the points at the largest values of \bar{y} (or u) deviate from the smooth growing of the points at smaller \bar{y} (or u), and they are not included on the fits. They are a reflection of the $2\pi/3L_t$ periodicity that we would see if we look at the phase diagram onto the constant β plane instead of onto the plane of constant x (see section 2). The data of Fig. 6 (especially those for $x = 1.0811$, for which many points of the phase transition line were determined) strongly suggest that there is

a cusp separating the β increasing curve from the β decreasing one. This means that the $2\pi/3L_t$ periodicity is realized by the periodic replication of a nonperiodic analytic function, producing a cusp at the points where a replica ends and a new replica starts. This cusp is a non-analyticity of the phase transition line which has the same origin as the Roberge-Weiss transition [13] found in QCD at $\mu = \pm i\pi/3L_t$ in the high temperature region [14]. Indeed, as it was conjectured in [15], this singular behavior realized as a cusp is to be expected in a wide variety of models characterized by a quantized charge coupled to a phase. In our case the quantized charge is the baryonic charge and the phase $\phi = \arctan(\bar{y}/x)$. Under this conditions, one must exclude the points to the right of the cusp from the fits since they belong to a different analytic function. Notice also that the presence of the nonanalytic cusp does not necessarily imply that the convergence radius of the Taylor series around $y = 0$ ($u = 1$) is limited by this singularity. Reference [15] contains a simple illustrative example on that in what we called gaussian model.

The transition lines displayed in Figures 5 and 6 are very smooth [they are essentially straight lines in the (u, β) plane until the cusp] and suggests a linear fit in the (u, β) plane. In fact the data reported in Table I imply actually a very high confidence level for the fits and to add higher order corrections, as for instance a quartic term in equation (10), seems meaningless. In other words, if higher order corrections were relevant at real y , it would be very hard to measure them from the data produced at imaginary y . This makes really difficult any serious analysis of systematic errors possibly induced by the fit ansatz.

Figure 7 displays the phase diagram in the plane $(\mu a, \beta)$, together with the results obtained by Fodor and Katz with double reweighting [2], and by D’Elia and Lombardo with imaginary chemical potential simulations [7]. There is good agreement with the results of Fodor and Katz until $\mu a \approx 0.3$, especially if we take into account that different methods to locate the pseudotransition coupling at finite volume are used. The agreement with D’Elia and Lombardo is very satisfactory in the whole range of μa explored. The main difference, which is already seen at $\mu a = 0$, should be attributed to a volume effect, since these authors used a $16^3 \times 4$ lattice. D’Elia and Lombardo give credit to their results for $\mu a \lesssim 0.3$, which is the interval where they found agreement with Fodor and Katz. We have seen that indeed the results (ours and theirs) are reliable at least until $\mu a = 0.5$, which is the maximum chemical potential at which we performed simulations. The disagreement with Fodor and Katz for $\mu a \gtrsim 0.3$ is likely due to the poor overlap of the ensemble of reweighted configurations with the ensemble of typical configurations at $\mu a \gtrsim 0.3$.

Figure 8 shows the phase diagram in the plane (μ, T) in physical units, with the scale set by the transition temperature at $\mu = 0$, T_C . The relative lattice spacings have been determined by means of the two loop beta function. For comparison, we also plot the result of D’Elia and Lombardo. Our results can be fit with a power function of the form

$$\frac{T}{T_C} = [1 - c(\mu/T_C)^2]^p . \quad (13)$$

The best χ^2 fit gives $c \approx 0.446(9)$ and an exponent, $p \approx 0.173(7)$. One may be curious about the extrapolation of this line to zero temperature. If this were done, we would find a zero temperature transition at chemical potential $\mu_C \approx 1.5T_C$, which, in terms of the nucleon mass [16], m_N , is $\mu_C \approx m_N/5$.

4 Conclusions

Using a recently proposed method to determine the phase transition lines at finite baryon density, we have obtained the phase transition line of QCD with four degenerate quark flavors from the zero density high temperature transition, at T_C , down to $T \approx 0.7T_C$ and $\mu \approx 1.4T_C$. Our results are in reasonably good agreement with those of D'Elia and Lombardo, obtained from simulations at imaginary chemical potential. These authors give credit to their results for $T \gtrsim 0.9T_C$, since this is the region where their results showed reasonably small statistical and systematic errors and in addition agree with those obtained by Fodor and Katz with the double reweighting method. Our results agree reasonably well with the central value reported by D'Elia and Lombardo in the whole region $T \gtrsim 0.7T_C$ and $\mu \lesssim 1.4T_C$.

We believe we can explore much lower temperatures with our method. Since it is based on analytical continuation/extrapolation there are uncontrolled systematic errors that grow in decreasing the temperature. It is therefore very difficult to estimate the minimum temperature at which our method will give a reliable prediction of the location of the phase transition point. In [10] we verified that in the three dimensional Gross-Neveu model at large N this minimum temperature is amazingly low.

The study of four flavor QCD thermodynamics at lower temperatures is very interesting, and we left it for future work. Since our method is computationally very expensive, we decided to concentrate the present effort in the more interesting cases of two and two plus one flavor QCD.

Acknowledgments

This work received financial support from CICYT (Spain), project FPA2003-02948, from Ministerio de Ciencia y Tecnología (Spain), project BFM2003-08532-C03-01/FISI, and from an INFN-CICYT collaboration. The authors thank the Consorzio Ricerca Gran Sasso that has provided most of the computer resources needed for this work. V.L. is a Ramón y Cajal fellow.

References

- [1] J.B. Kogut and M.A. Stephanov, *The Phases of Quantum Chromodynamics* (Cambridge University Press, 2004). J.B. Kogut, Nucl. Phys. (Proc.Suppl.) 119, 210-221 (2003).
- [2] Z. Fodor and S.D. Katz, Phys. Lett. B534, 87 (2002);
- [3] I.M. Barbour, S.E. Morrison, E.G. Klepfish, J.B. Kogut, and M.P. Lombardo, Nucl. Phys. B (Proc. Suppl.) 60A, 220 (1998).
- [4] Z. Fodor and S.D. Katz, JHEP 0203 (2002) 014; JHEP 0404 (2004) 050. Z. Fodor, S.D. Katz, and K.K. Szabo, JHEP 0405 (2004) 046.
- [5] E. Dagotto, A. Moreo, R.L. Sugar, and D. Toussaint, Phys. Rev. B41, 811 (1990). A. Hasenfratz and D. Toussaint, Nucl. Phys. B371, 539 (1992).

- [6] Ph. de Forcrand and O. Philipsen, Nucl. Phys. B642, 290 (2002); Nucl. Phys. B673, 170 (2003); Prog. Theor. Phys. Suppl. 153, 127-138, (2004).
- [7] M. D'Elia and M.P. Lombardo, Phys. Rev. D67, 014505 (2003); Phys.Rev. D70, 074509 (2004). M.P. Lombardo, Prog. Theor. Phys. Suppl. 153, 26-39 (2004).
- [8] C.R. Allton, S. Ejiri, S.J. Hands, O. Kaczmarek, F. Karsch, E. Laermann, C. Schmidt, and L. Scorzato, Phys. Rev. D66, 074507 (2002). C.R. Allton, S. Ejiri, S.J. Hands, O. Kaczmarek, F. Karsch, E. Laermann, and C. Schmidt, Phys. Rev. D68, 014507 (2003). C.R. Allton, M. Döring, S. Ejiri, S.J. Hands, O. Kaczmarek, F. Karsch, E. Laermann, and K. Redlich, hep-lat/0501030.
- [9] R.V. Gavai, S. Gupta, and R. Roy, Prog. Theor. Phys. Suppl. 153, 270 (2004). R.V. Gavai and S. Gupta, Phys. Rev. D68, 34506 (2003); hep-lat/0412035.
- [10] V. Azcoiti, G. Di Carlo, A. Galante, and V. Laliena, JHEP 1204 (2004) 010.
- [11] V. Azcoiti, G. Di Carlo, A. Galante, and V. Laliena, work in progress.
- [12] F.R. Brown, F.P. Butler, H. Chen, N.H. Christ, Z. Dong, W. Schaffer, L.I. Unger, and A. Vaccarino, Phys. Lett. B251, 181 (1990).
- [13] A. Roberge and N. Weiss, Nucl. Phys. B275, 734 (1986).
- [14] A. Hart, M. Laine and O. Philipsen, Phys. Lett. B505, 141 (2001).
- [15] V. Azcoiti, A. Galante, and V. Laliena, Prog. Theor. Phys. 109, 843 (2003).
- [16] K.D. Born, E. Laermann, N. Pirch, T.F. Walsh, and P.M. Zerwas, Phys. Rev. D40, 1653 (1989).

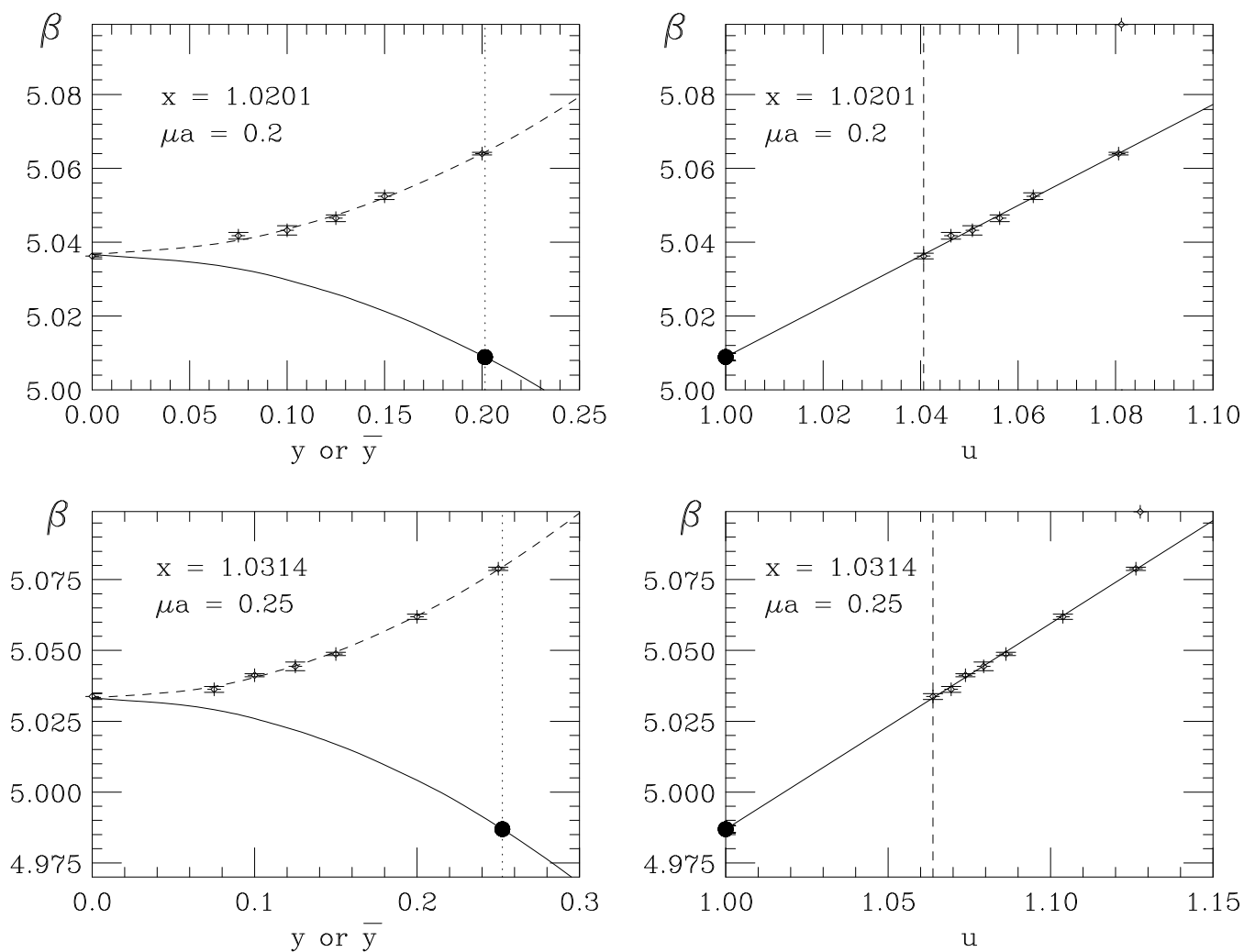


Figure 5: Phase diagrams at fixed x in the (\bar{y}, β) and (y, β) planes (left panels) and in the (u, β) plane (right panels).

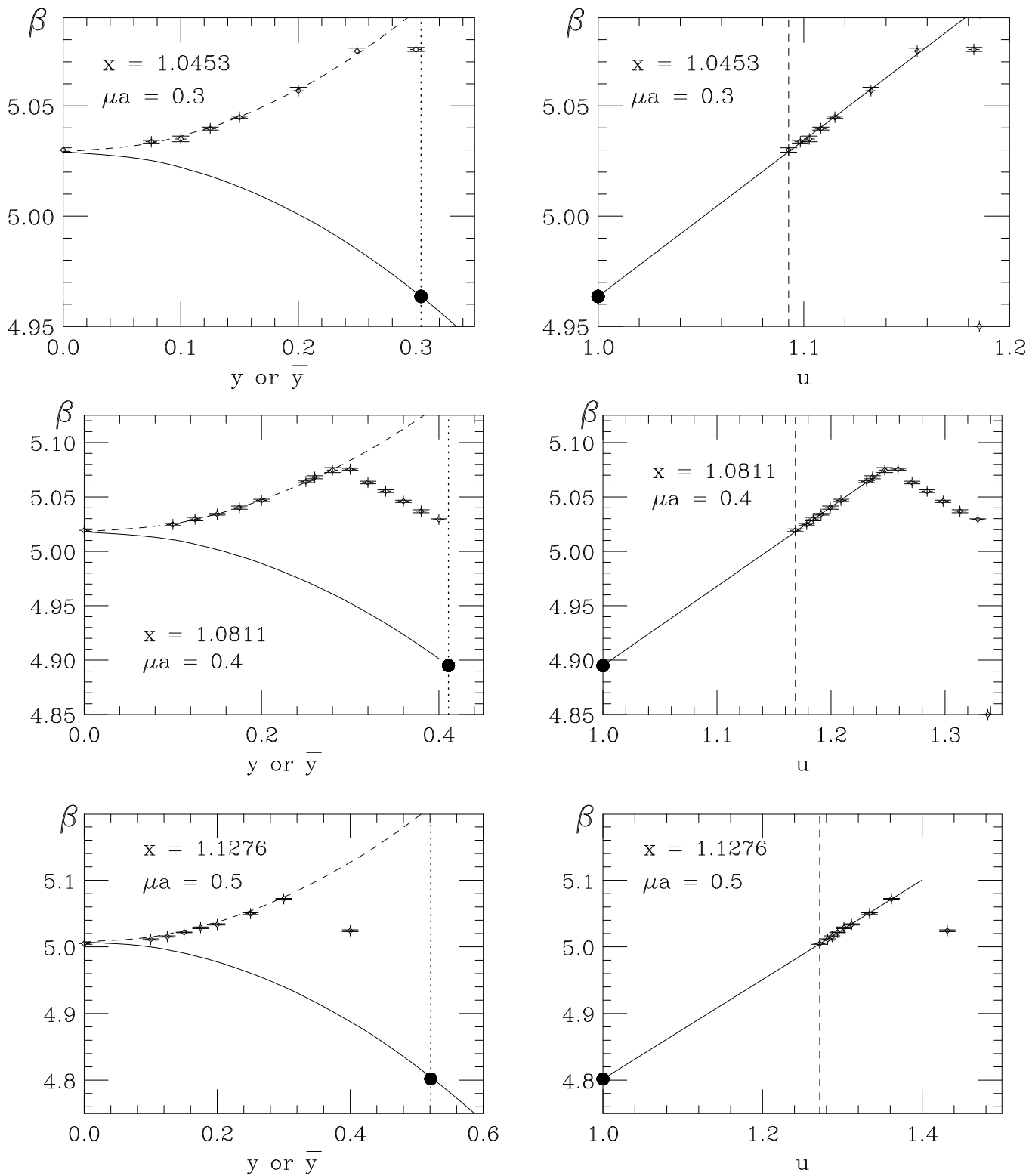


Figure 6: Phase diagrams at fixed x in the (\bar{y}, β) and (y, β) planes (left panels) and in the (u, β) plane (right panels).

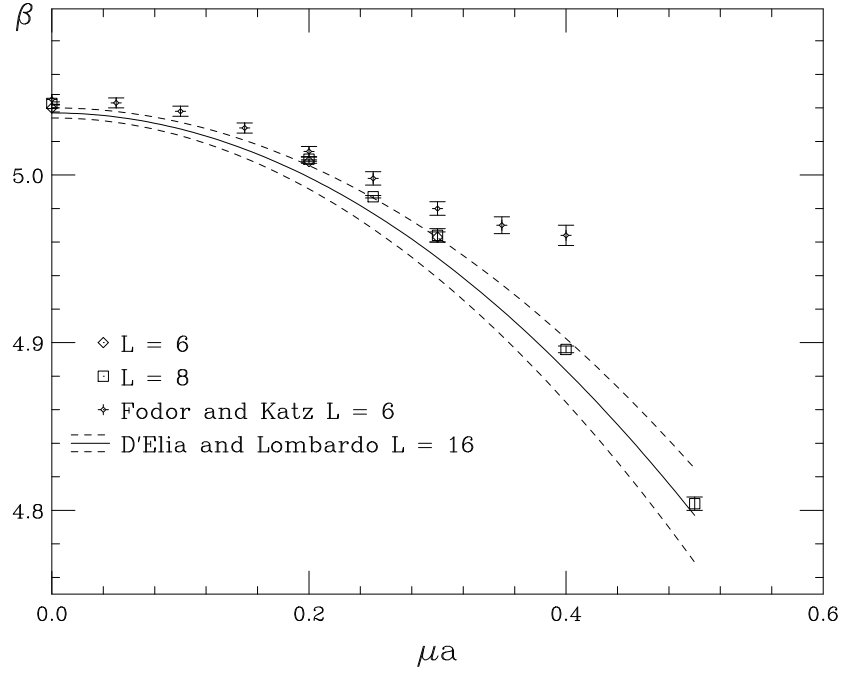


Figure 7: Phase diagram in the $(\mu a, \beta)$ plane. The solid line is the analytical continuation of the imaginary chemical potential pseudotransition line, and the dashed lines mark the error band. The authors of Ref. [7] give credit to this analytical continuation up to $\mu a \approx 0.3$.

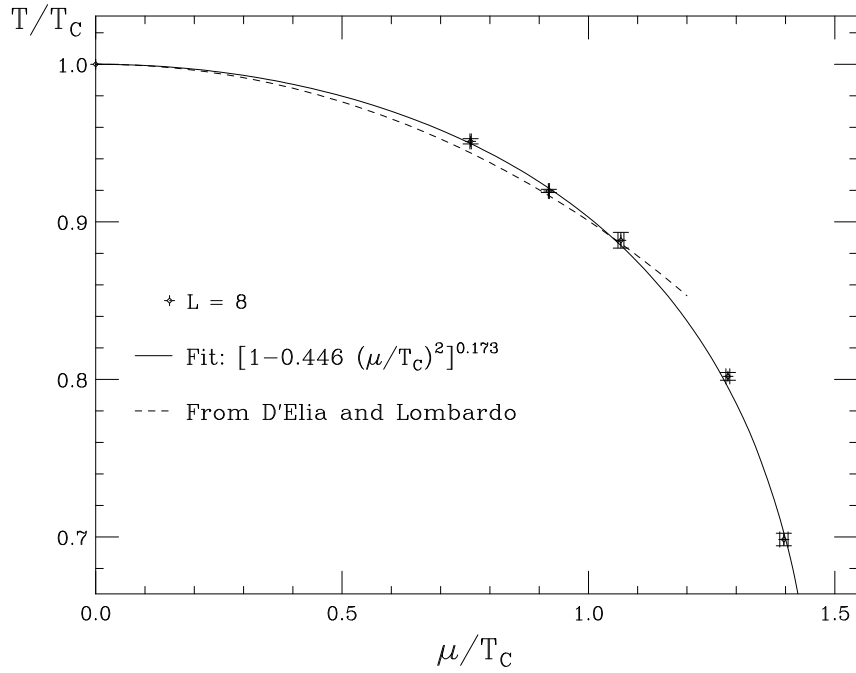


Figure 8: Phase diagram in physical units, with the zero density transition temperature, T_C , setting the scale.